Integrated Process-System Modeling and Performance Analysis for Serial Production Lines

Chen Li, Student Member, IEEE, Qing Chang*, Senior Member, IEEE, Guoxian Xiao, and Jorge Arinez, Member, IEEE

Abstract— The performance of a smart manufacturing system is affected by not only the constituent processes but also their system-level interactions. However, in most current studies, individual process modeling and system-level performance evaluation are independent. This can substantially impact production efficiency. In this paper, utilizing available sensor data, an integrated data-enabled model is developed to seamlessly fuse two conventionally separated system-level and process-level models and analysis. A fast recursive method is developed to evaluate the system yield. The permanent production loss (PPL) concept is defined and evaluated based on the proposed integrated model. Furthermore, PPL attributions due to random downtime and quality issues have been identified. Case studies have shown that the integrated model is of high fidelity, and the PPL analysis can effectively identify the root cause of production yield loss.

Index Terms—Intelligent and Flexible Manufacturing; Discrete Event Dynamic Automation Systems; Manufacturing, Maintenance and Supply Chains.

I. INTRODUCTION

Current manufacturing systems are increasingly complex, dynamic, and connected. The performance of a multi-stage manufacturing system is affected by individual process parameters (*process-level*) and interconnections among processes (*system-level*) [1] - [3]. To improve the throughput and product quality, substantial efforts have been devoted to process-level modeling (e.g., milling [4] and grinding [5], [6]) and system-level analysis and optimization [1], [7] - [9].

However, there has been a lack of a holistic model to integrate the two crucial aspects. The salient gap between the system-level and process-level analysis substantially impacts production efficiency. Take the crankshaft production line as an example. Each of the individual processes, e.g., grinding, achieves the highest quality and productivity by optimizing grinding operation parameters and related input variables (e.g., tool selection and condition). However, without

Manuscript received: February 26, 2022; Revised May 5, 2022; Accepted May 26, 2022.

This paper was recommended for publication by Editor Jingang Yi upon evaluation of the Associate Editor and Reviewers' comments. This work is supported by the National Science Foundation Grants CMMI 1853454.

C. Li and Q. Chang are with the Department of Mechanical and Aerospace Engineering, University of Virginia, Charlottesville, VA 22904, USA (email: cl4kv@virginia.edu and qc9nq@virginia.edu). G. Xiao and J. Arinez with General Motors R&D, General Motors Corporation, Warren, MI, 48090, USA (email: guoxian.xiao@gm.com,

and jorge.arinez@gm.com).

Digital Object Identifier (DOI): see top of this page

considering the overall system, such local process optimization might lead to an "overproduction" and overflow the downstream buffer. As a result, this effort not only does not contribute to improving the system throughput but also makes the parts stay in the buffer for a longer time, causing potential quality problems due to environmental conditions. From a system's point of view, speeding up individual processes may lead to the compounding effect of improving the overall production throughput. However, such requirements might not be feasible without knowing specific process constraints (e.g., tool life and part quality). This example illustrates the close-coupled interrelationship between process and system; namely, process-level performance directly impacts system-level performance and vice versa.

However, effective integration of processes and system is highly challenging. The conventional process-level performance is typically predicted by multi-physics analysis (e.g., heat transfer, mechanical deformation, etc.) using model-based simulation and/or experiments [10], [11]. In comparison, system-level performance evaluation is mainly concerned with the time-stamped material flow (e.g., throughput), and the current methods mostly focus on long-term steady-state performance based on simplified mathematical models (e.g., Markov chains) [12] – [15], or real-time performance analysis based on sensor data [8], [16]. Thus, the models and functions involved with the two levels, i.e., process and system, are vastly different.

With the increasingly available data at both the process and system levels, data-enabled approaches offer an unprecedented opportunity to tackle the integrated modeling problem. This paper aims to build an integrated data-enabled mathematical model that integrates process-level and system-level analysis to enable real-time production line analysis.

To this end, the contribution of this paper is threefold:1) Leveraging the sensor data, develop a novel process-system integrated data-enabled math model to incorporate process-level and system-level dynamics seamlessly, and a fast recursive algorithm to quickly evaluate both quality and quantity performance; 2) Develop a data-enabled analytical method to identify the real-time permanent production loss (PPL) efficiently; 3) Develop a PPL attribution method to identify the root cause and the problematic machines that are most responsible for production loss in a real-time fashion.

The remainder of the paper is organized as follows. Section II describes the production system to be analyzed. In Section

III, an integrated mathematical model is developed. A PPL identification and attribution methodology for a crankshaft line are proposed in Section IV. Numerical case studies demonstrated in Section V. Section VI summarizes the conclusion and future work.

II. SYSTEM DESCRIPTION

We intend to propose a formal integrated model for multistage production lines to include key process parameters and outputs in the system-level flow-based models. The integration requires a comprehensive understanding of specific manufacturing processes, such as grinding, milling, cutting, etc. Therefore, to make this paper concrete and more accessible, we adopt the grinding process for further formulation. We use a segment of a crankshaft line consisting of multiple consecutive grinding processes to illustrate the integrated process-system modeling methods. In addition, we use yield as the performance metric that can simultaneously consider production throughput and production quality. Yield is defined as the number of compliant products among total production outputs [2].

2.1. Grinding process description

Grinding is a commonly used process in finishing parts in numerous key manufacturing industry sectors such as aeronautical, automotive, and energy generation industries [17]. It directly impacts the functionality, dimensional accuracy, and surface integrity of the workpiece [18]. For the grinding process, thermal damage is one of the primary quality issues leading to defective products and further impacting the system yield. Thermal damage is caused by grinding burn, which occurs when the temperature of the workpiece in the grinding zone rises above the tempering temperature of the material due to inappropriate grinding parameters and leads to quality defects [17], [18]. Once the operating power exceeds a threshold power at a time point, a grinding burn will typically occur. We will adopt a wellaccepted grinding process model in [6] for the discussion. The threshold power at time t is given by the following equation

 $P_b(t) = 0.45u_{ch}(v_w(t)a(t)) + B(v_w^2(t)d_ea(t))^{\frac{1}{4}}$ (1) where $P_b(t)$ is the threshold power at time t, u_{ch} is the power for chip formation for steel, d_e is equivalent diameter, $v_w(t)$ is workpiece speed at time t, a(t) is the depth of cut at time t, and B is a constant related to burning temperature.

In order to avoid burning during the process, the grinding power P_{total} should not exceed its threshold P_b . Thus, the actual grinding power at time t is formulated as [6]:

$$P_{total}(t) = u_{ch}\left(v_w(t)a(t)\right) + 4\mu p_0 v_w(t) \left(\frac{a(t)}{d_e}\right)^{\frac{1}{2}} A_{eff} (2)$$

where μ is friction coefficient, and p_0 is the contact pressure, A_{eff} is effective wheel wear flat area (dullness), which is a function of V_w , and $V_w(t)$ is the number of parts processed by each station since the previous dressing. Dressing refers to a periodical treatment for the grinding wheels to remove the current abrasive layer so that a new and sharp surface is

exposed to the work surface.

Therefore, at station S_i , if $P_{totoal,i} > P_{b,i}$, the workpiece will have thermal damage and will be removed from the grinding station. Otherwise, if $P_{totoal,i} \le P_{b,i}$, the workpiece will have no thermal damage and will be delivered to the next grinding station.

2.2. Model description and notation

This paper considers a serial production line (such as a crankshaft line), as shown in Fig. 1, which includes M stations, M virtual buffers to store damaged workpieces, and M-1 inline buffers for compliant workpieces. Stations are represented by rectangles, and buffers are represented by circles. Since the defective parts will be dislodged right away from their corresponding station, virtual storage buffers with infinite capacity are attached to each station for modeling purposes. The virtual storage buffers serve as counters for the defects at each station.

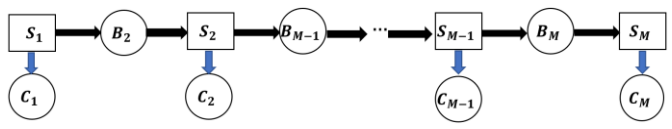


Fig. 1. The structure of serial production lines with virtual storage buffers. The following notations are adopted in this model:

- 1) S_i denotes the i^{th} station, where i = 1, 2, ..., M.
- 2) $v_{w,i}(t)$ denotes the workpiece speed of station S_i at time t, where i = 1, 2, ..., M.
- 3) $a_{w,i}(t)$ denotes the depth of cut of station S_i at time t, where i = 1, 2, ..., M.
- 4) $G_i(t)$ indicates stock removal of station S_i at time t, where i = 1, 2, ..., M.
- 5) b is the workpiece width.
- 6) $V_{w,i}(t)$ is the number of parts produced since the previous dressing for station S_i at time t, where i = 1, 2, ..., M.
- 7) $T_i(t)$ represents the real-time cycle time for station S_i at time t, where i = 1, 2, ..., M.
- 8) Each inline buffer has a finite capacity. B_i denotes i^{th} buffer's capacity, where i = 2, 3, ..., M.
- 9) $b_i(t) = [b_2(t), b_3(t), ..., b_M(t)]'$ are the buffer levels at time t.
- 10) $C_i(t) = [C_1(t), C_2(t), ..., C_M(t)]'$ are the number of defects, i.e., thermal damaged workpieces, at each station at time t.
- 11) $\vec{e}_i = (j, t_i, d_i)$, denotes a disruption event that j^{th} station S_j is down at time t_i with time duration of d_i , where $i = 1, 2, ..., n_r$, j = 1, 2, ..., M. $E = [\vec{e}_1, ..., \vec{e}_n]$, denotes a sequence of disruption events.
- 12) S_{M^*} denotes the slowest station of the production line, and T_{M^*} denotes the cycle time of the slowest station.

The following assumptions are also made to clarify the system.

1) A station is blocked if it is operational, and its downstream buffer is full, as well as its downstream machine is down.

- A station is starved if it is operational, and its upstream buffer is empty, as well as its upstream machine is down.
- 3) When the i^{th} station S_i is neither blocked nor starved at time t; it will run at its real-time rated speed $v_i(t) = 1/T_i(t)$, which is dependent on process-level control parameters.

III. DATA-ENABLED INTEGRATED MODEL

Our previous study [8] has developed a data-enabled system-level model to account for the real-time production output of serial production lines. In this paper, we will integrate the process-level model (i.e., grinding process as an example) and the system-level dynamic model by extending our previous data-enabled model. This integrated model takes both system-level and process-level parameters as inputs, and outputs will be the system yield. Thus, the integrated model considers quantity (based on system-level material flow) and quality (based on the grinding process model addressing threshold power). Therefore, to embed the process level knowledge, the state space equation of the integrated process-system can be written as:

$$\dot{X}(t) = F(X(t), V_w(t), G(t), v_w(t), a(t), C(t), W(t))$$
(3)
$$Y(t) = H(X(t))$$
(4)

In the context of this manufacturing system, the physical meaning of each component could be described as follows:

- $X(t) = [X_1(t), X_2(t), ..., X_M(t)]'$, where $X_i(t)$ denotes the total production counts of station S_i up to time t.
- Y(t) is the system yield, which denotes the number of compliant productions from the end-of-line station S_M up to time t.
- $F(*) = [f_1(*), f_2(*), ..., f_M(*)]'$, where $f_i(*)$ is the system dynamic function of station S_i .
- $W(t) = [W_1(t), W_2(t), ..., W_M(t)]'$ is the system status variable at time t, where $W_i(t)$ denotes whether station S_i is suffering a disruption event at time t. If a random disruption event $\exists \vec{e}_k \in E.s.t.\vec{e}_k = (i, t_k, d_k)$ and $t \in [t_k, t_k + d_k]$, then, $W_i(t) = 1$, otherwise, $W_i(t) = 0$.
- $C(t) = [C_1(t), C_2(t), ..., C_M(t)]'$, where $C_i(t)$ denotes the accumulated defects coming from station S_i at time t.
- $v_w(t) = [v_{w,1}(t), v_{w,2}(t), ..., v_{w,M}(t)]'$ denotes the workpiece speed at each station at time t.
- $a(t) = [a_1(t), a_2(t), ..., a_M(t)]'$ represents the depth of cut for each station at time t.
- $G(t) = [G_1(t), G_2(t), ..., G_M(t)]'$ is the stock removal for each station up to time t.
- $V_w(t) = [V_{w,1}(t), V_{w,2}(t), ..., V_{w,M}(t)]'$ is the number of parts processed by each station since the previous dressing.

According to the process model, the cycle time of station S_i is assumed to be controllable and is a function of process-level control parameters at time t as:

level control parameters at time
$$t$$
 as:
$$T_i(t) = \frac{G_i(t)}{v_{w,i}(t)a_{w,i}(t)b}$$
(5)

We define the accumulated defects between two stations S_i and S_i within a time period [0, t] as $C_{ij}(t)$:

$$C_{ij}(t) = \begin{cases} -\sum_{k=j}^{i-1} C_k(t) + \sum_{k=j}^{i-1} C_k(0), & i > j \\ \sum_{k=i}^{j-1} C_k(t) - \sum_{k=i}^{j-1} C_k(0), & i < j \end{cases}$$
(6)

According to the conservation of the flow, the accumulated total production difference between two machines S_i and S_j $(\forall i, j \in [1,2,...,M], i \neq j)$ at any time t could be represented as:

$$X_{i}(t) - X_{j}(t) = \begin{cases} \sum_{k=j+1}^{i} b_{k}(0) - \sum_{k=j+1}^{i} b_{k}(t) + C_{ij}(t), i > j \\ \sum_{k=i+1}^{j} b_{k}(t) - \sum_{k=i+1}^{j} b_{k}(0) + C_{ij}(t), i < j \end{cases}$$
(7)

Therefore, the buffer conditions between stations S_i and S_j at time $t: X_i(t) - X_j(t) - C_{ij}(t)$ are bound by the condition that all buffers between machine S_i and S_j are full (for i < j) or empty (for i > j). Denote the boundary as β_{ij} , we have

$$\beta_{ij} = \begin{cases} \sum_{k=j+1}^{i} b_k(0), & i > j \\ \sum_{k=i+1}^{j} B_k - \sum_{k=i+1}^{j} b_k(0), & i < j \end{cases}$$
 (8)

Thus, $X_i(t) - X_j(t) - C_{ij}(t) \le \beta_{ij}$ Considering the interactions between S_i and S_j , in the case of $X_i(t) - X_j(t) - C_{ij}(t) < \beta_{ij}$, station S_i is neither starved or blocked by S_j ; thus, it will process parts at its own rated speed. If $X_i(t) - X_j(t) - C_{ij}(t) = \beta_{ij}$, the processing speed of station S_i will be constrained by station S_j . Define a segment function $\xi(u,v)$ as $\xi(u,v) = \begin{cases} +\infty, & u < 0 \\ v, & u = 0 \end{cases}$, The actual processing speed of station S_i can be described as: $\dot{X}_i(t) = \frac{1}{2} \sum_{i=1}^{N} (t_i) - \frac{1}{2} \sum_{i=1}^{N} (t_i$

$$\min \left\{ \frac{\xi \left(\left(X_{i}(t) - X_{j}(t) - C_{ij}(t) \right) - \beta_{ij}, 1 - W_{j}(t) \right) \left(v_{w,j}(t) a_{w,j}(t) b \right)}{G_{j}(t)}, \frac{(1 - W_{i}(t)) (v_{w,i}(t) a_{w,i}(t) b)}{G_{j}(t)}, \right\}$$
(9)

Extend this equation to all stations in the system, then, $\dot{\mathbf{y}}'(t) =$

$$\min \left\{ \begin{array}{c} \frac{\xi\Big(\big(X_i(t) - X_1(t) - C_{i1}(t)\big) - \beta_{i1} \big), 1 - W_1(t))(v_{W,1}(t) a_{W,1}(t)b)}{G_1(t)}, \\ \vdots \\ \frac{\big(1 - W_i(t)\big) \big(v_{W,i}(t) a_{W,i}(t)b\big)}{G_i(t)}, \\ \vdots \\ \frac{\xi((X_i(t) - X_M(t) - C_{iM}(t)) - \beta_{iM}), 1 - W_M(t))(v_{W,M}(t) a_{W,M}(t)b)}{G_M(t)} \end{array} \right\}$$

$$= f_i(\mathbf{X}(t), \mathbf{V}_{\mathbf{w}}(t), \mathbf{G}(t), \mathbf{v}_{\mathbf{w}}(t), \mathbf{a}(t), \mathbf{C}(t), \mathbf{W}(t))$$
(10)

In addition, V_w as an input variable for calculating the grinding power, it is vital to embed it in the integrated model. V_w denotes the number of parts processed by each station since the previous dressing. If a dressing takes place at time t, $V_{w,i}$ is reset to 0, i.e., $V_{w,i}(t+1) = 0$.

To summarize all stations, the state space function is:

$$X(t) = \begin{bmatrix} f_1(X(t), V_w(t), G(t), v_w(t), a(t), C(t), W(t)) \\ \vdots \\ f_M(X(t), V_w(t), G(t), v_w(t), a(t), C(t), W(t)) \end{bmatrix}$$

$$= F(X(t), V_w(t), G(t), v_w(t), a(t), C(t), W(t)) \qquad (11)$$

$$Y(t) = X_M(t) - C_M(t) = H(X(t)) \qquad (12)$$

The buffer levels of a certain buffer B_{i+1} at time t could be calculated as:

$$b_{i+1}(t) = X_i(t) - X_{i+1}(t) + b_{i+1}(0) - C_i(t) + C_i(0)$$
 (13)

Therefore, up to time t, given the sensor data of random disruption events E, the control parameters $v_{w,i}(t)$, $V_{w,i}(t)$, $G_i(t)$, $a_i(t)$, and the initial buffer levels $b_i(0)$, the system state at any given time can be recursively evaluated by Eqs. (11) - (13).

It is worth emphasizing that the control parameters, namely $v_{w,i}(t)$, $V_{w,i}(t)$, $G_i(t)$, $a_i(t)$, not only determine the overall production output and material flow as shown in Eqs. (5) - (7), but also define the quality performance at each station as shown in Eq. (1). Together, they incorporate process-level and system-level performance represented as system yield.

IV. PERMANENT PRODUCTION LOSS DIAGNOSIS

To measure the real-time performance of the production line, it is necessary to understand and quantify the impact of disturbance and quality issues on the system. A station's random downtime may cause a halt in production at one station, thus starving downstream stations or blocking upstream stations. In addition, the defects also result in a production loss to the system. In this paper, permanent production loss (PPL) is introduced as a quantitative measurement of the impact on a serial production line due to disruption events and quality issues. The overall permanent production loss is defined as the qualified production difference between the real serial production line and the ideal serial production line. The ideal serial line is defined as a virtual production line that does not suffer from any disruption event (e.g., station's random failure). It does not have any quality issues (i.e., no defect). The ideal serial line presents the best possible system performance. Definition 1 makes the PPL more accurate.

Definition 1: Given a realization of a production line subject to a sequence of disruption events $E = [\vec{e}_1, ..., \vec{e}_n]$ and a sequence of quality problems $\mathbf{Q} = [q_1, ..., q_n]$, the overall permanent production loss of a serial production line during [0,T] is defined as the difference between the yields of the ideal serial line, denoted as $Y_{ideal}(T)$, and the real-time yields $Y(T; E, \mathbf{Q})$, that will never recover in any circumstances, i.e., $PPL(T) = Y_{ideal}(T) - Y(T; E, \mathbf{Q})$ (14)

Permanent production loss is an important indicator to evaluate the performance of the production line in real-time operation. As shown in Definition 1, both disruption events and quality issues will result in PPL to the production line. We will discuss the evaluation and attribution of PPL due to disruption events (PPL_E) and PPL due to quality issues (PPL_B) in the following sub-sections.

4.1. PPL_E Identification and Attribution

4.1.1. PPL_E Identification

Definition 2: Given a realization of a production line subject to a sequence of disruption events $E = [\vec{e}_1, ..., \vec{e}_n]$ and a sequence of quality problem $Q = [q_1, ..., q_n]$ during a period [0, T], the permanent production loss due to disruption events (PPL_E) is

$$PPL_E(T) = Y_{clean}(T; \mathbf{Q}) - Y(T; \mathbf{E}, \mathbf{Q})$$
 (15) where $Y(T; \mathbf{E}, \mathbf{Q})$ and $Y_{clean}(T; \mathbf{Q})$ are the yields of the serial production line with and without disruption events $\mathbf{E} = [\vec{e}_1, ..., \vec{e}_n]$.

In order to evaluate PPL_E , it is necessary to identify the impact of station stoppages on the system performance. Because of finite inline buffer capacities and variations in processing times of different stations, a disruption event does not necessarily lead to a permanent system production loss. The opportunity window serves as a measurement of the system status directly related to the resilience to disruption events. Our previous study [8] has defined the concept of opportunity window and PPL_E for the system with variable cycle time machines. We will extend these concepts and develop PPL_E evaluation methods for a serial line to embed the process level knowledge. The summary of the related basic concepts is provided without detailed proof to make the paper self-contained.

Opportunity window of a station S_j , denoted as $OW_j(T_d)$, is the longest possible downtime on S_j at time T_d that would not result in permanent production loss at the end-of-line station. It can be defined as:

$$OW_i(T_d) = \sup \{ \geq 0 : s.t. \exists T^*(d),$$

$$\int_0^T s_M(t)dt = \int_0^T \tilde{s}_M(t; \vec{e})dt, \forall T \ge T^*(d)$$
 (16)

where $\int_0^T \tilde{s}_M(t; \vec{e}) dt$ and $\int_0^T s_M(t) dt$ are the production volume of the end-of-line station S_M at time T, with and without disruption event $\vec{e} = (m, T_d, d)$, respectively, $T^*(d)$ signifies the potential dependency of T^* on d.

We proposed a method in [8] to segment a time horizon into a sequence of time intervals and considered OW and PPL_E within the small time period, and then aggregate them. We adopt the same idea in this paper. First, we define the real-time slowest station $S_{M^*}(t)$ as the station has the largest cycle time $T_{M^*}(t)$ at time t. Then, for this integrated model, the cycle time of the slowest station at time t is:

$$T_{M^*}(t) = \max_{i=1,\dots,M} \frac{G_i(t)}{v_{w,i}(t)a_{w,i}(t)}$$
(17)

Assume that the slowest station switches K times during a time interval [0,T] and denote the time point when the slowest station switches as t_k , k=1,2,...,K. We can segment the time [0,T] into a sequence of time intervals $[t_k,t_{k+1}], k=1,2,...,K$.

Assume that a downtime event $\vec{e} = (j, t, d)$ occurs during [0, T], if the slowest station switches k times during the time interval [0, T], then its opportunity window during each segmented interval can be represented as:

$$OW_j(t) = T_{M^*}(t_k) (X_j(t) - X_{M^*}(t) - C_{jM^*}(t) + \beta_{j,M^*})$$
(18) for $\forall t \in [t_k, t_{k+1})$.

Assume that a downtime event $\vec{e} = (j, t, d)$ occurs during [0, T]. The permanent production loss due to stations' random failures can be represented as the summation of production loss within each slowest station switching interval, such that:

$$PPL_{\vec{e}}(T) = \int_{0}^{T} s_{j}(t')dt' - \int_{0}^{T} s_{j}(t', \vec{e})dt'$$

$$= \sum_{k=1}^{K} \frac{d_{z} - OW_{j}(tt_{k})}{T_{M^{*},k}}, \forall T > T^{*}$$
(19)

4.1.2. PPL_E Attribution

To further identify the impact of each station's downtime on the production line yields, the PPL_E needs to be attributed to individual stations. Based on our integrated data-enabled model, the real-time states X(t), B(t), and C(t) from each station can be evaluated by using Eqs. (11) - (13). We adopt the same idea and segment the time interval $[t_a, t_b]$ to a sequence of intervals $[t_k, t_{k+1}), k = 0, 1, 2, ..., K$, where t_k is the time point when the slowest station switches, and $t_0 = t_a$, $t_{K+1} = t_b$. Let $T_{M^*,k}$ denote the corresponding cycle time of the real-time slowest station at time t_k , and $OW_i(t_k)$ be the opportunity window at time t_k .

We first discuss single disruption event $\vec{e}_1 = (j, t_1, d_1)$ occurring during the time interval $[t_a, t_b]$. For each of the slowest station switching interval $[t_k, t_{k+1})$, the slowest station remains the same. Thus, the PPL_E due to \vec{e}_1 during single slowest station switching interval is:

$$PPL_{\vec{e}_{1}}[t_{k}, t_{k+1}] = \max \left\{ 0, \frac{t_{k+1} - t_{k}}{T_{M^{*}, k}} - X_{j}(t_{k}) + X_{M^{*}}(t_{k}) + C_{jM^{*}}(t) - \beta_{j, M^{*}} \right\} (20)$$

If there are two disruptions $\vec{e}_1 = (j_1, t_1, d_1)$ and $\vec{e}_2 =$ (j_2, t_2, d_2) occurring during $[t_k, t_{k+1})$, the PPL_E can be attributed to the disruption event whose corresponding machine has a smaller opportunity window. If the opportunity window is equal, we attribute the production loss evenly to \vec{e}_1 and \vec{e}_2 .

The PPL_E analysis can be extended to a general case with multiple disruption events $\vec{E} = [\vec{e}_1, ..., \vec{e}_n]$ occurring during a period $[t_a, t_b]$. PPL_E due to a disruption event $\vec{e}_i =$ $(j_i, t_i, d_i), 1 \le i \le n$, during $[t_k, t_{k+1}]$ is:

$$\begin{split} PPL_{\vec{e}_i}[t_k, t_{k+1}] &= \\ \left(\max\{0, \frac{t_{k+1} - t_k}{T_{M^*,k}} - \left(X_{j_i}(t_k) - X_{M^*}(t_k) - C_{jM^*}(t_k) + \beta_{j_i,M^*} \right) \right) \end{split}$$

 $\left\{\frac{\max\{0,\frac{t_{k+1}-t_k}{T_{M^*,k}}-\left(X_{j_i}(t_k)-X_{M^*}(t_k)-C_{jM^*}(t_k)+\beta_{j_i,M^*}\right)}{\rho},cond.A\right\}$

where condition A is

where condition A is
$$\min \begin{cases} X_{j_1}(t_k) - C_{j_1M^*}(t_k) + \beta_{j_1,M^*} \\ \vdots \\ X_{j_n}(t_k) - C_{j_nM^*}(t_k) + \beta_{j_n,M^*} \end{cases} = X_{j_i}(t_k) - C_{j_iM^*}(t_k) + \beta_{j_i,M^*}$$

 ρ is the total number of stations satisfying the condition during $[t_k, t_{k+1}]$, while condition B is

$$\min \begin{cases} X_{j_1}(t_k) - C_{j_1M^*}(t_k) + \beta_{j_1,M^*} \\ \vdots \\ X_{j_n}(t_k) - C_{j_nM^*}(t_k) + \beta_{j_n,M^*} \end{cases} \\ < X_{j_i}(t_k) - C_{j_iM^*}(t_k) + \beta_{j_i,M^*} \end{cases}$$

Therefore, the PPL_E attributed to the disruption event \vec{e}_i (j_i, t_i, d_i) , $1 \le i \le n$, during time period $[t_a, t_b]$ can be summarized as:

$$PPL_{\vec{e}_i}[t_a, t_b] = \sum_{k=1}^{K} PPL_{\vec{e}_i}[t_k, t_{k+1}]$$
 (22)

The PPL_E can be further attributed to each station. Given a sequence of disruption events that occur at station S_i denoted as $\vec{e}_{j,1}, \dots, \vec{e}_{j,n}$ during the period [0,T], the permanent production loss caused by downtime events of S_i within [0, T]can be deduced as:

$$PPL_{E,j}[0,T] = \sum_{a=1}^{n} PPL_{\vec{e}_{j,n}}$$
 (23)

4.2. PPL_a Identification and Attribution

For a serial production line, defects will be dislodged from the system. Thus, these defects are also permanently lost to the production line due to quality issues.

Definition 3: Given a realization of a production line subject to a sequence of disruption events $E = [\vec{e}_1, ..., \vec{e}_n]$ and a sequence of quality problem $\mathbf{Q} = [q_1, ..., q_n]$ during a period [0,T], the permanent production loss due to quality issue (PPL_a) is

$$PPL_{a}(T) = Y_{h\nu}(T; \mathbf{E}) - Y(T; \mathbf{E}, \mathbf{Q})$$
 (24)

where $Y(T; \mathbf{E}, \mathbf{Q})$ and $Y_{hy}(T; \mathbf{E})$ are the yields of the serial production line with and without quality problems Q = $[\vec{q}_1, ..., \vec{q}_n].$

As we discussed in Section 2.1, a part is burned at station S_i if $P_{total,i}(t) > P_{b,i}(t)$. The burned parts will be immediately taken away from S_i and delivered to its storage buffer C_i . The accumulated defects attributed to station S_i up to time *T* is denoted as:

$$PPL_{q,j}(T) = C_j(T) \tag{25}$$

Therefore, the overall permanent production loss (PPL) attributed to station S_i up to time T, can be summarized as:

$$PPL_{i}(T) = PPL_{E,i}(T) + PPL_{a,i}(T)$$
 (26)

V. CASE STUDY

This section provides case studies to demonstrate: 1) the high fidelity of the proposed integrated data-enabled model and the associated recursive calculation method in evaluating system yield, and 2) the effectiveness of permanent production loss attribution methods in identifying the root cause of performance inefficiency. The following case studies compare a serial line's production counts and inline buffer levels from the proposed integrated model and simulation experiment. In addition, two experiments are conducted to demonstrate that the proposed system performance (PPL) attribution methods are effective.

To make the proposed integrated model and PPL

attribution method easy to follow in a real-world application, a flow chart is presented in Fig. 2. As shown in Fig. 2, the stock removal G(t), depth of cut a(t), workpiece's speed $v_w(t)$, number of parts processed $V_w(t)$, and the downtime recording W(t) are inputs collected from the real plant floor sensor data. With these inputs for the integrated model, the real-time processing speed $\dot{X}(t)$ of each grinding machine and the stepwise PPL_E can be evaluated by Eq. (10) and Eq. (21), respectively. Then, based on the quality inspection method discussed in Section 2.1 and Eq. (11), the system yields X(t) and accumulated defects C(t) can be recursively calculated. As described in Section 4.2, C(t) is the PPL caused by the quality issue. Meanwhile, the PPL due to downtime events $PPL_E(t)$ and its attribution to each station can also be identified with the recursive method.

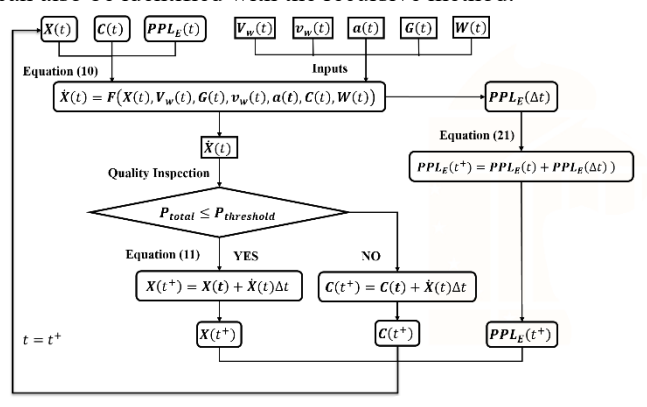


Fig. 2. The flow chart of the integrated model application.

To make the Validation generally reliable, 100 numerical experiments are conducted on different process lines with various parameters. For demonstration purposes, we will present case studies on a segment of a crankshaft line that consists of four grinding stations, four virtual buffers for damaged workpieces, and three inline buffers similar to Fig. 1.

The process-level and system-level parameters for each grinding station and the system-level buffer parameters are shown in Table I and Table II, respectively. The dressing action is executed when a grinding station has processed 1000 parts. In the experiments, these parameters are based on a real crankshaft line. However, we only show the mocked parameters and data for confidential consideration. In addition, we allow the control input, workpieces speed v_w , varies within 10% of its original speed at each station based on a random policy to mimic the real production line operation, where the workpiece speed can be adjusted.

Table I. Parameters for the grinding stations

Station	S_1	S_2	S_3	S_4
Original workpiece speed (mm/s)	115	115	115	115
Depth of cut (mm)	0.1	0.06	0.025	0.015
Designed stock removal (mm ³)	1.5	0.9	0.45	0.15

Workpiece width (mm)	22	22	22	22
MTBF (min)	500	600	450	600
MTTR (min)	20	15	15	26

Table II. Parameters of the inline buffers

Buffer	B_2	B_3	B ₄
Initial buffer level	5	9	6
Buffer capacity	12	30	20

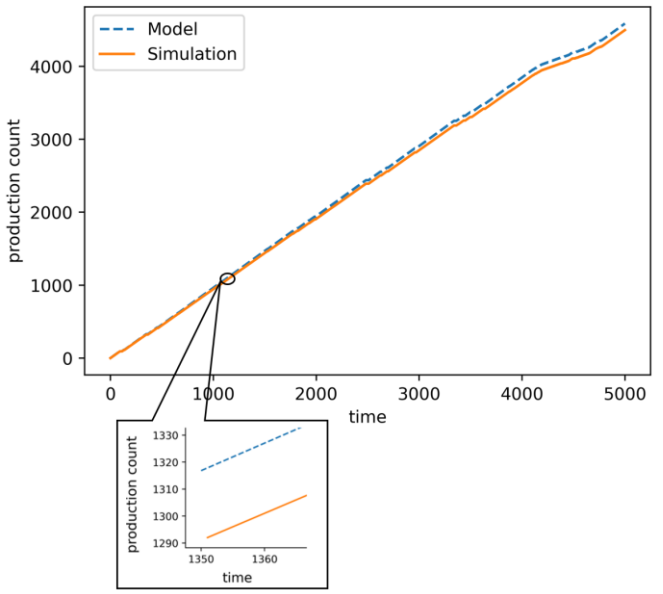
5.1. Fidelity of the integrated data-enabled model

For validation purposes, the output from the proposed integrated modeling and the recursive algorithm is compared with that from a simulation. We adopt a discrete event simulation software, Simul8, to perform the simulation.

The simulation duration is one week, i.e., 5000 minutes, assuming 12 operation hours a day. The production counts and buffer levels derived from the proposed recursive calculation method are compared with the simulation results.

The results are evidence that the production counts of each station and buffer levels of each buffer obtained by using the proposed integrated data-enabled model and recursive calculation are in high agreement with that derived from the simulation. For demonstration purposes, only the output of the end-of-line stations S_4 and the buffer level of the last inline buffer B_4 are shown in Fig. 3 and Fig. 4, respectively. The results from the integrated data-enabled model ("blue-dash line") and the results from the simulation ("red-solid line") are almost overlapped with each other in the figures. A more precise detail can be found in the zoom-in window for both figures.

Based on the comparison results of all samples, the average value of the maximum absolute errors of these 100 lines between the integrated model and simulation is 3.16%. Thus, the integrated process-system model is considered to be accurate.



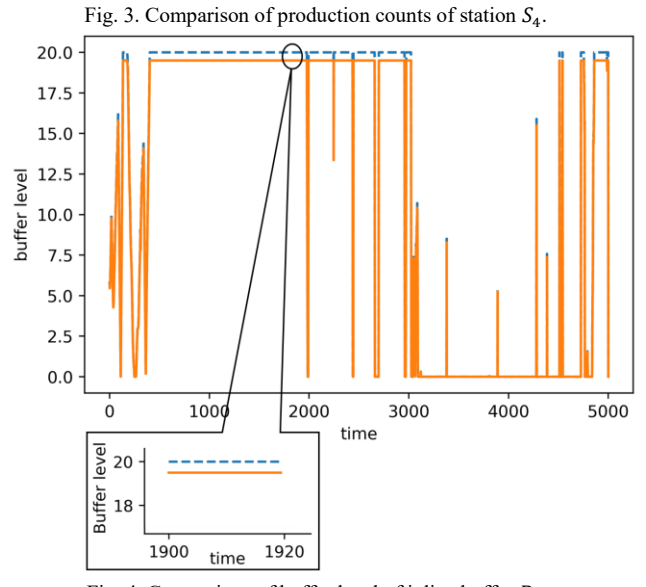


Fig. 4. Comparison of buffer level of inline buffer B_4 .

5.2. PPL Identification and Attribution

Based on the integrated model, we further evaluate PPL and attribute the PPL_E and PPL_q to each station with the proposed methods in Section IV. As shown in Fig. 5, the overall PPL can be attributed to either random downtime (redshaded bars) or thermal damage (green-shaded bars) at every station. The PPL attribution provides a natural ranking of stations with problematic issues, i.e., machine reliability (related to random downtime) or inappropriate process parameter settings (related to thermal damage). With this, production control and maintenance activities can be prioritized appropriately, which will be our future work. In this paper, we only focus on PPL analysis, and we will validate whether the attribution of PPL_E and PPL_q to each station are correct based on our proposed methods.

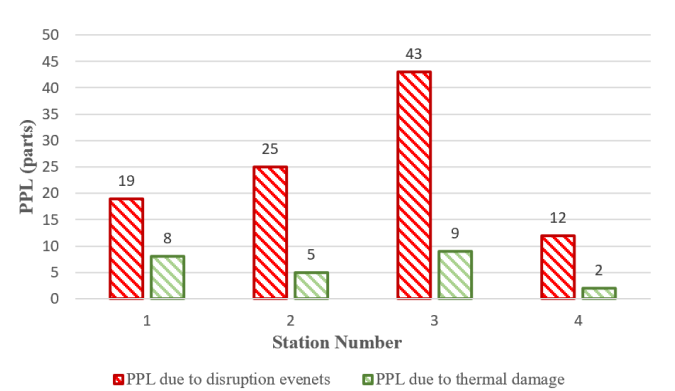


Fig. 5. PPL distribution for each station.

5.2.1. Validation of PPL_E Attribution

The PPL_E attribution to a specific station is a part of the overall production output loss caused by that station due to the downtime events. Therefore, if we remove all the downtime events on that station while keeping other conditions unchanged, we should expect that the overall production output is increased by an amount close to the

attributed PPL_E amount, assuming the proposed method is effective.

A series of controlled experiments are performed to validate the accuracy of the PPL_E attributions. We first obtain the PPL_E attributions to each disruption event, and then aggregate to each grinding station based on Eqs. (22) – (23). The PPL_E attribution result is shown as red shaded bars in Fig. 5. Then, in simulation, we observe a production output increase by removing all the disruption events at each station one at a time. The output improvement results of the controlled experiments using simulation are shown as bluecheckboard bars in Fig. 6.

The result shows that the PPL_E attribution is in close agreement with the overall productivity improvement in the corresponding controlled simulation experiments. Hence, the proposed method is proved to be accurate in quantifying and ranking each station's influence on the permanent production losses due to downtime events.

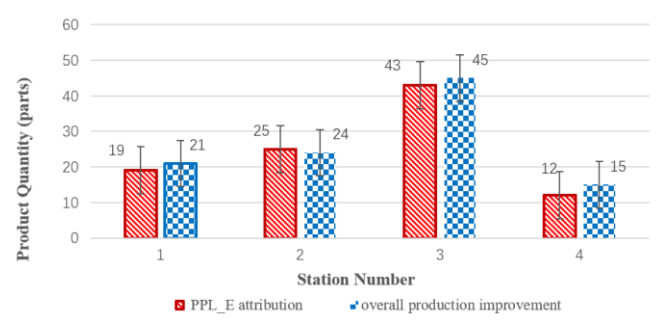


Fig. 6. Overall production improvement and PPL_E distribution.

5.2.2. Validation of PPL_q Attribution

Once the real-time grinding power exceeds its threshold, thermal damage (burn) will happen to the part. The defects attributed to each station is the number of burned parts stored in the associated virtual buffer for defects.

Therefore, the production output should increase if we ignore the thermal damage caused by a grinding station and deliver all parts to its downstream buffer. The increased amount should be close to the defects distributed to that station. A series of controlled experiments are carried out. We first obtain the defects of each grinding station by applying the proposed method, which is shown as green-shaded bars in Fig. 7. Then, in simulation, we ignore the thermal damage caused by each grinding station one at a time to evaluate the additional output due to the neglect of the burned parts. The simulation results of the controlled experiments are shown as blue-checkerboard bars in Fig. 7.

The result shows that the defects attribution is in close agreement with the extra output due to the neglect of the burned parts in the corresponding controlled simulation experiment. We can conclude that the proposed method is accurate in each station's contribution to permanent production losses due to thermal damage.

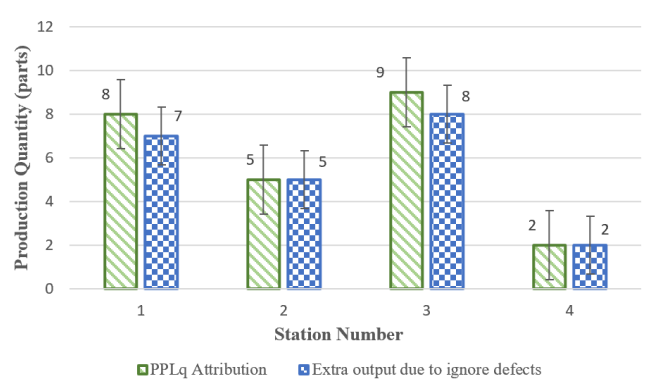


Fig. 7. Extra output due to ignore burned parts and defects distribution.

VI. CONCLUSION AND FUTURE WORK

In this paper, a process-system integrated data-enabled model is built to incorporate the system-level and process-level dynamics for a serial production line. The permanent production loss due to both disruption events and quality issues is identified based on the proposed model. In addition, the PPL attribution to each station caused by different issues can be quantified. In the future, we will design control policies based on this integrated model and PPL analysis to adjust each station's process parameters to improve overall production performance.

REFERENCES

- J. Li, & S. M. Meerkov, Production systems engineering. (Springer US, 2009). doi:10.1007/978-0-387-75579-3.
- [2] J. Huang, J. Zhang, Q. Chang, R. X. Gao, Integrated process-system modelling and control through graph neural network and reinforcement learning, CIRP Annals, Volume 70, Issue 1, 2021, Pages 377-380, ISSN 0007-8506, https://doi.org/10.1016/j.cirp.2021.04.056
- [3] W. Shi, J. Stream of Variation Modeling and Analysis for Multistage Manufacturing Processes. Stream of Variation Modeling and Analysis for Multistage Manufacturing Processes, CRC press, 2010. doi:10.1201/9781420003901
- [4] D. Huo, W. Chen, X. Teng, C. Lin, & K. Yang, Modeling the influence of tool deflection on cutting force and surface generation in micromilling. *Micromachines* 8, (2017).
- [5] S. Liang, J. A. Shih, S. Y. Liang, & A. J. Shih, Grinding Processes. in Analysis of Machining and Machine Tools 45–62 (Springer US, 2016). doi:10.1007/978-1-4899-7645-1 4.
- [6] G. Xiao, S. Malkin, On-Line Optimization for Internal Plunge Grinding, CIRP Annals, Volume 45, Issue 1, 1996, Pages 287-292, ISSN 0007-8506, https://doi.org/10.1016/S0007-8506(07)63065-0.
- [7] B. Waschneck, A. Reichstaller, L. Belzner, T. Altenmüller, T. Bauernhansl, A. Knapp, & A. Kyek, Optimization of global production scheduling with deep reinforcement learning. *Procedia CIRP* 72, 1264–1269 (2018).
- [8] C. Li, J. Huang and Q. Chang, "Data-Enabled Permanent Production Loss Analysis for Serial Production Systems with Variable Cycle Time Machines," in *IEEE Robotics and Automation Letters*, vol. 6, no. 4, pp. 6418-6425, Oct. 2021, doi: 10.1109/LRA.2021.3093012.
- [9] M. Ghahramani, Y. Qiao, M. C. Zhou, A. O'Hagan and J. Sweeney, "AI-based modeling and data-driven evaluation for smart manufacturing processes," in *IEEE/CAA Journal of Automatica Sinica*, vol. 7, no. 4, pp. 1026-1037, July 2020, doi: 10.1109/JAS.2020.1003114.
- [10] J. Wiley & Sons, Fundamentals of Modern Manufacturing: Materials, Processes, and Systems, Groover MP. Fundamentals of modern manufacturing: materials, processes, and systems, 7th Edition. 2020 Jul 15.
- [11] J. Liu, Z. Zhao, C. Tang, C. Yao, C. Li and S. Islam, "Classifying Transformer Winding Deformation Fault Types and Degrees Using FRA Based on Support Vector Machine," in *IEEE Access*, vol. 7, pp. 112494-112504, 2019, doi: 10.1109/ACCESS.2019.2932497.

- [12] L. G. Curry and M. R. Feldman, "Manufacturing systems modeling and analysis," Manufacturing Systems Modeling and Analysis, Springer-Verlag Berlin Heidelberg 2009. doi: 10.1007/978-3-540-88763-8.
- [13] Y. Dallery, & B. S. Gershwin, Manufacturing flow line systems: a review of models and analytical results. Queueing Syst, 1992, doi:10.1007/BF01158636.
- [14] Z. Jia, L. Zhang, J. Arinez and G. Xiao, "Finite Production Run-Based Serial Lines with Bernoulli Machines: Performance Analysis, Bottleneck, and Case Study," in *IEEE Transactions on Automation Science and Engineering*, vol. 13, no. 1, pp. 134-148, Jan. 2016, doi: 10.1109/TASE.2015.2433674.
- [15] Z. Jia & L. Zhang, "Serial production lines with geometric machines and finite production runs: performance analysis and system-theoretic properties," International Journal of Production Research, 57:8, 2247-2262, 2019, doi: 10.1080/00207543.2018.1513658
- [16] J. Zou, Q. Chang, Y. Lei and J. Arinez, "'Production system performance identification using sensor data", IEEE Trans. Syst. Man Cybernet. Syst., vol. 48, no. 2, pp. 255-264, Feb. 2018.
- [17] I. Pombo, L. Godino, J. A. Sánchez, R. Lizarralde. Expectations and limitations of Cyber-Physical Systems (CPS) for Advanced Manufacturing: A View from the Grinding Industry. *Future Internet*. 2020; 12(9):159. https://doi.org/10.3390/fi12090159
- [18] F. Klocke, S.L. Soo, B. Karpuschewski, J.A. Webster, D. Novovic, A. Elfizy, et al. Abrasive machining of advanced aerospace alloys and composites. CIRP Ann Manuf Technol, 64 (2015), pp. 581-604